ICES Journal of Marine Science, 2023, **0**, 1–15
DOI: 10.1093/icesjms/fsad024
Original Article

ICES CIEM International Council for the Exploration of the Sea
Conseil International pour l'Exploration de la Mer

Transport-driven seasonal abundance of pelagic fishes in the Chukchi Sea observed with seafloor-mounted echosounders

R. M. Levine [1,2,*], A. De Robertis [1], D. Grünbaum [2] and C. D. Wilson [1,#]

[1]Alaska Fisheries Science Center, National Marine Fisheries Service, National Oceanic and Atmospheric Administration, 7600 Sand Point Way NE, Seattle, Wa, 98115, USA
[2]School of Oceanography, University of Washington, 1501 NE Boat St, Seattle, WA 98195, USA

[*] *Corresponding author. tel: +1 206 526 4337;* e-mail: Robert.Levine@noaa.gov.
[#]Retired

Recent summer surveys of the northeastern Chukchi Sea found pelagic fishes were dominated by large numbers of age-0 Arctic cod (*Boreogadus saida*, Gadidae) and walleye pollock (*Gadus chalcogrammus*, Gadidae), while adult fishes were comparatively scarce. The source and fate of these young fishes remain unclear, as sampling in this region is impeded by seasonal ice cover much of the year. Seafloor-mounted echosounders were deployed at three locations in the northeastern Chukchi Sea from 2017 to 2019 to determine the movement and seasonal variability of these age-0 gadids. These observations indicated that the abundance of pelagic fishes and community composition on the Chukchi Sea shelf were highly variable on seasonal time scales, with few fish present in winter. Tracking indicated that fish movements were strongly correlated with local currents. Fishes were primarily displaced to the northeast in summer and fall, with periodic reversals towards the southwest driven by changes in regional wind patterns. The flux of fishes past the moorings indicated that the prevailing northward currents transport a large proportion of the age-0 pelagic fishes present on the Chukchi shelf in summer to the northeast by fall, leading to relatively low abundances of age-1+fishes in this environment.

Keywords: Arctic cod, *Boreogadus saida*, echosounder, *Gadus chalcogrammus*, mooring, polar cod, transport, walleye pollock.

Introduction

The shallow continental shelf of the Chukchi Sea is covered by sea ice in late winter and spring until warm water from the south initiates the retreat of the ice in spring (Woodgate *et al.*, 2010). The retreating ice leads to a largely ice-free Chukchi Sea during the summer. Seasonal sea ice extent in the Chukchi has declined over recent decades (Frey *et al.*, 2015) and is predicted to continue to decrease at a rate of 0.94 d year^{-1} (0.11–1.55, Wang *et al.*, 2018) as temperatures in the region increase (Danielson *et al.*, 2020). These changes are expected to alter the ecology of endemic Arctic fishes (Mueter *et al.*, 2021): further intrusion of boreal species will likely displace the southern boundary of Arctic species northward, altering the structure and components of the local food web (Marsh and Mueter, 2020).

Age-0 gadids, particularly Arctic cod (*Boreogadus saida*), dominate the pelagic fish community on the Chukchi shelf in the summer (De Robertis *et al.*, 2017). Arctic cod is a circumpolar species found throughout the Arctic basin and surrounding shelves (Lowry and Frost, 1981; Rand and Logerwell, 2011; De Robertis *et al.*, 2017; Mecklenburg *et al.*, 2018), where they are a key pelagic component of energy transfer between lower and upper trophic levels (Whitehouse *et al.*, 2014). While large numbers of age-0 Arctic cod have been observed in the Chukchi in the summer, adults are comparatively scarce (De Robertis *et al.*, 2017; Levine *et al.*, 2023). The observed population of adult Arctic cod lacks the reproductive potential to produce the population of age-0 fish on the shelf during summer (Marsh *et al.*, 2020). Thus, these age-0 fish likely originated elsewhere. Based on modelling studies of larval dispersal, it is likely that these age-0 Arctic cod may originate in the southern Chukchi or northern Bering Seas in winter and early spring (Deary *et al.*, 2021; Vestfals *et al.*, 2021), where spawning may occur under seasonal sea ice (Ponomarenko, 2000).

The pelagic fish assemblage on the Chukchi shelf has undergone rapid changes as the ecosystem warms. Boreal species such as walleye pollock (*Gadus chalcogrammus*) comprise an increasing portion of the summer age-0 gadid community in the eastern Chukchi Sea (Wildes *et al.*, 2022; Levine *et al.*, 2023). In the Bering Sea to the south, the distribution of adult pollock has shifted north as a result of warming, with high densities of mature adults in the northern Bering Sea in recent years (Stevenson and Lauth, 2019; Eisner *et al.*, 2020). Eggs and larvae from this northern Bering Sea population are likely to be transported north along with the movement of water through the Bering Strait onto the Chukchi shelf (Figure 1, Woodgate *et al.*, 2005). Thus, age-0 pollock in the Chukchi Sea are hypothesized to originate from this large population of adult fish south of the Bering Strait (Levine *et al.*, 2023).

The Chukchi shelf is hypothesized to be an important nursery area for these age-0 gadids in summer (De Robertis *et al.*, 2017; Levine *et al.*, 2021), when relatively warm temperatures support high growth rates for both Arctic cod and pollock (Laurel *et al.*, 2018). Such conditions are necessary to maximize growth prior to experiencing winter conditions. How-

Received: November 1, 2022. **Revised:** February 7, 2023. **Accepted:** February 8, 2023

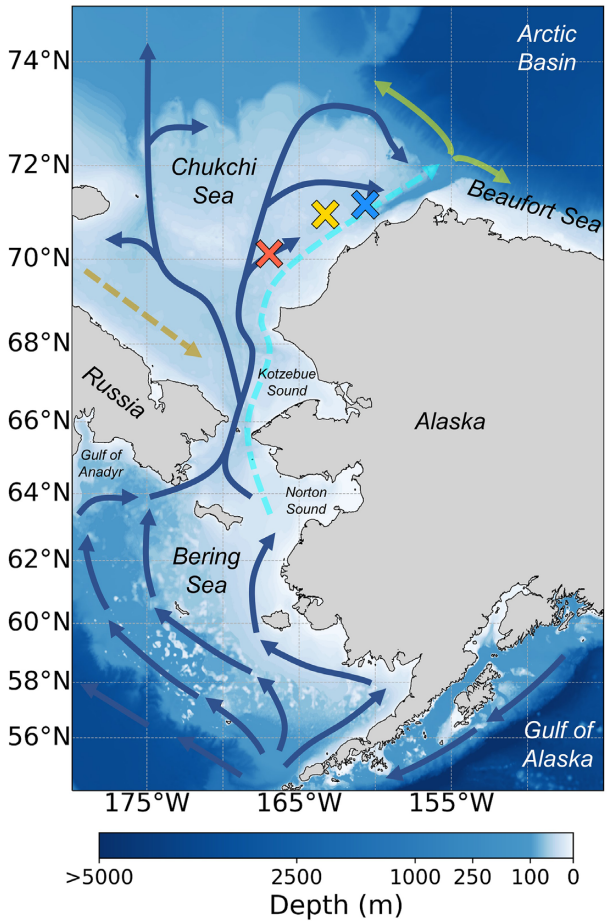

Figure 1. Map of the study region. The locations of the southern (red), central (yellow), and northern (blue) mooring sites are indicated by an X. The primary annual mean transport pathways through the Bering and Chukchi seas identified in Weingartner *et al.*, (2005) and Corlett and Pickart, (2017) are shown: Alaskan Coastal Current (light blue), Bering Sea water (dark blue), Siberian Coastal Current (yellow), slope current (green, westward), and shelf break jet (green, eastward). Dashed lines indicate seasonal currents.

ever, it remains unclear whether the abundant age-0 fishes observed in the summer provide recruits to other areas, or the Chukchi Sea is an ecological sink where most of the age-0 fish do not survive the winter (De Robertis *et al.*, 2017). Growth and metabolic demands of age-0 gadids are largely temperature-dependent (Laurel *et al.*, 2018). Therefore, the potential success of populations on the Chukchi shelf may initially depend on their movement into suitable nursery grounds during the summer feeding season, and subsequently depend on movement into environments conducive to winter survival.

Advection from the south structures the distribution of the planktonic communities in the Chukchi in summer (Eisner *et al.*, 2013; Danielson *et al.*, 2017; Pinchuk and Eisner, 2017; Spear *et al.*, 2020). The predominant northward currents are also hypothesized to transport gadid larvae into the Chukchi Sea (Vestfals *et al.*, 2019; Vestfals *et al.*, 2021). Repeat surveys and transport simulations in 2018 indicated that advection played a key role in the distribution of larger, more motile, age-0 gadids on the Chukchi shelf in late summer (Levine *et al.*, 2021). Periods of on-shelf retention of the population were likely important for growth for these small fishes, prior to their being transported northwards towards the Beaufort Sea and Central Arctic Basin in the fall (Levine *et al.*, 2021). Modelling studies have hypothesized that the northward advection determines the distribution of age-0 fishes observed in summer (Deary *et al.*, 2021; Vestfals *et al.*, 2021). However, these model predictions assume that behaviour has a negligible influence on transport. There are no direct observations establishing whether the large numbers of age-0 gadids observed in summer migrate to other areas or this region serves as a sink with fishes remaining in the area but failing to survive through the winter. If advection is the primary mechanism for large-scale fish movements, measurements or model predictions of currents may provide opportunities to predict changes in the distribution of these age-0 fishes on the Chukchi shelf.

Direct observations of fishes in ice-covered areas have been restricted both spatially and temporally as traditional trawling gear cannot be used (Lønne and Gulliksen, 1989; Gradinger and Bluhm, 2004; Melnikov and Chernova, 2013). Acoustic backscattering observations of pelagic fishes have been collected from icebreakers (Benoit *et al.*, 2008) or autonomous underwater vehicles operating under sea ice (Fernandes *et al.*, 2003) to monitor fishes during periods of ice cover. Specialized net systems designed to sample along the ice edge have made it easier to collect specimens under sea ice over a greater area (Flores *et al.*, 2012; David *et al.*, 2016). However, these methods are logistically difficult and expensive as they rely on ice-capable ships. Additionally, the deployment of underwater vehicles or nets in ice-covered areas is typically limited to a few discrete locations and relatively short periods of time.

In contrast, moored instrumentation can be deployed during the ice-free period and left to collect data year-round. Acoustic Doppler Current Profilers (ADCP, Wallace *et al.*, 2010) and echosounders (Miksis-Olds *et al.*, 2013; Darnis *et al.*, 2017; Kitamura *et al.*, 2017; Gonzalez *et al.*, 2021) have been used to study zooplankton and fish presence during extended periods of ice cover. However, moorings have not been previously used to collect long-term observations of fish movements through ice-covered regions. Moored echosounders can be used to collect continuous data to study fish abundance (Trevorrow, 2005; Urmy *et al.*, 2012; De Robertis *et al.*, 2018). Acoustic split-beam observations make it possible to track the positions of individuals over successive pings, which can then be used to infer swimming speed and direction (Ehrenberg and Torkelson, 1996). This detection of individual scatterers can also be used to infer the size composition, transport, and behaviour of fishes from moored platforms (Kaardvedt *et al.*, 2009). Acoustic observations offer limited capacity to discriminate among taxa. However, in low-diversity regions where backscatter is well-classified and dominated by a single species or species group, acoustic data can be used to infer information about the population as the interpretation of these data are less dependent on the collection of biological samples (De Robertis *et al.*, 2018; Levine *et al.*, 2021).

This study is based on two years of near-continuous acoustic observations of age-0 gadids from seafloor-mounted echosounders at three sites in the northeastern Chukchi Sea. The primary objectives were to characterize the seasonal patterns in pelagic fish abundance in the Chukchi Sea, and to determine the roles of advective transport and fish behaviour in the movement of age-0 gadids. Year-round observations enabled us to characterize the seasonal changes of the pelagic ecosystem to better constrain the possible fate of the large juvenile population of fishes present during the summer months.

Methods

Mooring deployments

Three moorings were deployed in the northeastern Chukchi Sea in locations where high fish densities had been observed in the summer (De Robertis *et al.*, 2017). The moorings were deployed for two years as part of the North Pacific Research Board's Arctic Integrated Ecosystem Research Program (Baker *et al.*, 2020) at 71.03 N, 160.50 W (49 m depth, hereafter referred to as northern); 70.83 N, 163.11 W (44 m depth, hereafter referred to as central); and 70.01 N, 166.85 W (47 m depth, hereafter referred to as southern) (Figure 1). The moorings were deployed between 8 and 15 August 2017, recovered and redeployed between 12 and 15 August 2018 (after data download and maintenance), and recovered again between 26 August and 5 September 2019.

Composition of acoustic scatterers

The low-diversity pelagic fish community of the Chukchi shelf simplifies the process of making biological inferences from measurements of acoustic backscatter. Four acoustic-trawl surveys, in which daytime acoustic backscatter was partitioned based on the selectivity-corrected catch of the nearest trawl (see De Robertis *et al.*, 2017 for details), were conducted in the northeastern Chukchi Sea since 2012. Surveys in 2012 and 2013 identified age-0 Arctic cod as the primary biological scatterers in summer (mean length of 3.5 cm, De Robertis *et al.*, 2017). Surveys using the same methods during the mooring deployment period in summer 2017 and 2019 similarly indicated that age-0 Arctic cod and walleye pollock were the dominant pelagic scatters, accounting for 93.0 and 88.3% of the 38 kHz backscatter in 2017 and 2019, respectively, (mean lengths of ~4–5 cm, Levine *et al.*, 2023). Age-0 Arctic cod and pollock are difficult to distinguish morphologically, and genetic analyses were used to confirm the proportion of pollock during these surveys (Wildes *et al.*, 2022). Thus, both age-0 Arctic cod and walleye pollock were likely abundant throughout the 2017–2019 mooring deployment period. Other pelagic fishes such as capelin (*Mallotus villosus*) and Pacific herring (*Clupea pallasii*) were present in comparatively low abundances and were estimated to account for <6% of integrated acoustic backscatter during summer surveys in both 2017 and 2019 (Levine *et al.*, 2023), consistent with the previous observations in 2012 and 2013 (De Robertis *et al.*, 2017). While their total abundances varied over the eight-year period, age-0 gadids were the dominant contributor to pelagic backscatter across the four years of surveys (Levine *et al.*, 2023). Therefore, during the summer and fall periods of the mooring deployments, there is strong evidence that the primary contributors to backscatter were age-0 gadids, and that acoustic-based measures of density during this period reflect the abundance and distribution of age-0 Arctic cod and walleye pollock combined. However, the composition of pelagic scatterers at other times of the year remains poorly understood. Thus, we used the acoustic properties of the scatterers to infer transitions in the composition of the pelagic community throughout the time series.

Mooring instrumentation

The mooring platforms were designed to be low profile to maximize the range of water column sampled by the echosounder and to minimize the likelihood of damage due to sea ice. They were instrumented with battery-powered scientific echosounders (Wideband Autonomous Transceiver, Simrad AS). Each transceiver operated a 70 kHz, 18° split-beam transducer (ES70-18CD), positioned upward in a two-axis gimbal equipped with a 0.7 kg counterweight (Supplementary Figure S1). In addition, each transceiver also operated a combined 38 kHz 18° split-beam and 200 kHz 18° single-beam transducer (ES38-18/200–18C) fixed to the grating. Both transducers were positioned at a height of 0.8 m above the seafloor. During the deployment, the echosounders transmitted a group of 300 pings (200 pings at 70 kHz followed by 100 pings at 38 and 200 kHz) at a ping rate of 0.4 s every 2 h, hereafter referred to as an ensemble. Data were recorded to a range of 60 m to ensure data collection past the range of the sea surface (a depth range of 44.4–49.0 m for all deployments). The echosounders were calibrated at the surface using a 38.1-mm tungsten carbide sphere, following the standard sphere method (Demer *et al.*, 2015; Renfree *et al.*, 2019). The echosounders used in 2017–2018 were calibrated prior to deployment. The echosounders used in 2018–2019 were calibrated following recovery because the transducers recovered in summer 2018 were immediately redeployed. The echosounder recovered at the southern mooring site in 2019 could not be calibrated due to instrument damage associated with recovery. The average gains from the five calibrations of the other instruments were used for data processing along with the factory-specified beamwidths for the transducers. Overall, the gains among all instruments were relatively consistent; the average gains for each frequency were 19.12 (±0.80 SD) dB at 38 kHz, 19.98 (±0.86 SD) dB at 70 kHz, and 17.98 (±0.55 SD) dB at 200 kHz. However, these calibrations did not account for potential pressure effects. Preliminary field experiments using three of the deployed echosounders indicate that at 70 kHz (ES70-18CD transducers), the average target strength (*TS*) of a calibration sphere varied by <0.4 dB re 1 m^2 (i.e. <10% in linear units) at deployment depths of 40–50 m relative to measurements collected at the surface.

To determine the heading of the transducers when settled on the seafloor, each mooring was deployed with a calibrated compass mounted at a fixed position aligned with the forward direction of the transducers. Deployments used either a custom magnetometer designed by the Engineering Development division of NOAA's Pacific Marine Environmental Laboratory, or an Aaronia GPS Logger sealed in a pressure housing. The compass recordings confirmed that mooring orientations were stable throughout the deployment (Supplementary Figure S2). The mode of all observations collected after deployment, corrected for magnetic declination at each site, was used to represent the mooring orientation (Supplementary Table S1).

Acoustic data processing

Acoustic data were recorded from 8 August 2017 to 26 August 2019 at the southern site, 9 August 2017 to 4 September 2019 at the central site, and 15 August 2018 to 5 September 2019 at the northern site. The northern mooring site did not record data for the 2017–2018 deployment, likely due to a configuration error. In addition, the 38 kHz transducer at the central mooring site failed during the 2018–2019 deployment. Thus, only the 70 and 200 kHz data were included in the analyses. Interference (likely from side-lobe reverberation) appeared consistently at 16–20 and 27–30 m depth at

200 kHz at the central mooring site during the 2018–2019 deployment. Only data within those ranges, where the signal was 10 dB higher than the observed noise level were used in the analyses.

Acoustic data were processed using Echoview 12.0 (Echoview Software Pty Ltd). The depth of the sea surface/ice echo was determined by Echoview's threshold offset operator with a minimum detection threshold of -50 S_v (dB re 1 m^{-1}) below the surface/ice, and manually corrected after visual inspection. Volume backscatter (S_v, dB re 1 m^{-1}) at 70 and 200 kHz and the nautical area scattering coefficient (s_A, m^2 nmi^{-2}; MacLennan *et al.*, 2002) at 70 kHz were integrated in 1 m bins from 2 m above the transducer to 2 m below the sea surface/ice echo for every ensemble without integration thresholds. To investigate the impact of diel vertical migration on observed integrated backscatter, the solar altitude at each ensemble was determined as a function of datetime and location using the Pysolar library for Python (http://pysolar.org).

Fish tracking and flux estimates

Echoes from individual scatterers were identified with Echoview's split-beam single target detection (method 2), using a detection threshold of -70 dB re 1 m^2 in order to restrict detection to fish-like scatterers (Supplementary Table S2). Single targets were joined into individual track trajectories using Echoview's 4D alpha-beta tracker (Blackman, 1986; see Supplementary Table S3 for parameters used in this study). A minimum of five detections from an individual was required to classify a track, with a maximum gap of five pings (2 s). The mean *TS* (dB re 1 m^2) of each track was calculated as $10log_{10}(\bar{\sigma}_{bs})$ where $\bar{\sigma}_{bs}$ (m^2) is mean backscattering cross section (i.e. the averaged linear form of *TS*, MacLennan *et al.*, 2002). Given that the objective was to determine the net horizontal displacement of tracks, headings, and speeds were calculated in 2D by first fitting linear models with respect to time for the x, y positions of the single target detections in each track. Heading was calculated from the linear model predictions as $tan^{-1}(\frac{y_{t_n}-y_{t_0}}{x_{t_n}-x_{t_0}})$, where t_0 and t_n are the first and last time points of the track, respectively (where tan^{-1} represents the 2-argument arctangent to account for the sign of both x and y). Horizontal speed was calculated by dividing the total distance along the model-fit linear track $\sqrt{(x_{t_n}-x_{t_0})^2+(y_{t_n}-y_{t_0})^2}$ by the duration of the track. Headings were converted from a coordinate system relative to the transducer into a geographic reference frame based on the compass orientation.

Density (A, individuals m^{-2}) was calculated using the 70 kHz observations at each ensemble (200 pings at 70 kHz every 2 h) as $A = s_A/(4\pi\bar{\sigma}_{bs} \times 1852^2)$ following MacLennan *et al.*, (2002). The vertically integrated flux of individuals (Q, ind. m^{-1} s^{-1}) was estimated using the density and mean speed and direction of tracks during each ensemble, such that $Q_U = AU$ and $Q_V = AV$, where U and V are the mean of the zonal (east-west) and meridional (north-south) velocity components of all tracks within each ensemble, respectively. Thus, Q_U and Q_V represent the number of individuals per second in the entire water column moving towards the east and north, respectively, underneath a 1 m line of the sea surface. Throughout each mooring deployment (i), the mean direction (θ_i), and flux (Q_i) was calculated using the mean of the zonal and meridional flux estimates as

$$\theta_i = tan^{-1}\left(\frac{\bar{Q}_V}{\bar{Q}_U}\right)$$

and

$$Q_i = \sqrt{\bar{Q}_U^2 + \bar{Q}_V^2},$$

where tan^{-1} represents the 2-argument arctangent. The net movement of individuals during each mooring deployment M_i was then estimated as $M_i = Q_i T_i$ where T is the total duration of the mooring deployment in seconds.

Detecting shifts in community composition

The frequency-dependence of backscatter can be used to differentiate among key groups of scatterers (Jech and Michaels, 2006; De Robertis *et al.*, 2010; Benoit-Bird and Lawson, 2016). Greater backscatter at 200 kHz than at 70 kHz is indicative of weakly scattering targets, such as zooplankton lacking gas inclusions, while gadids exhibit greater backscatter at 70 kHz than at 200 kHz (De Robertis *et al.*, 2010). Similarly, *TS* is species- and size-dependent (McClatchie *et al.*, 1996; Benoit-Bird and Lawson, 2016) and has been used to distinguish the age-0 gadids that are prevalent in the Pacific Arctic from zooplankton and other weaker scatterers (Geoffroy *et al.*, 2016).

Given that the composition of pelagic scatterers in winter is unknown, we calculated what fraction of the total backscatter and flux in each deployment occurred when $\Delta S_{v,70\text{-}200\,kHz}$ and *TS*s were consistent with scattering from fishes. During the period of acoustic-trawl surveys in August and September of 2017 and 2019 in which juvenile gadids were found to dominate the backscatter (Levine *et al.*, 2023), the mean $\Delta S_{v,70–200}$ of the mooring observations was > -3 dB in 94.1% of ensembles, with a median of 2.7 dB (calculated from 2394 of 22660 ensembles, Supplementary Figure S3a). In the same ensembles, the median *TS* was -54.0 dB re 1 m^2, and 95.3% of ensembles had a mean *TS* > -62 dB re 1 m^2 (calculated from 24346 tracks in 2394 of 22660 ensembles, Supplementary Figure S3b). This corresponds to the lower bound of *TS* expected for small age-0 Arctic cod and is consistent with *TS* values used to differentiate fish and zooplankton scatterers in previous studies of the Pacific Arctic pelagic environment (-65 dB re 1 m^2, Benoit *et al.*, 2014; Geoffroy *et al.*, 2016). Given that trawl sampling during the surveys indicate that fish, in particular gadids, dominated the backscatter during these periods, thresholds of $\Delta S_{v,70–200}$ > -3 dB and *TS* > -62 dB re 1 m^2 were considered indicators for periods when backscatter was dominated by fish.

Environmental data

Bottom temperature and salinity were measured using a conductivity, temperature, and depth (CTD, Sea-Bird Scientific SBE-37) sensor mounted on each mooring (Supplementary Figure S1). Hourly current measurements were derived from ADCPs (Teledyne RD Instruments WorkHorse operating at either 300 or 600 kHz) deployed <500 m from the echosounder moorings and averaged into 60 min and 4 m bins (Stabeno and McCabe, 2023). To investigate the relationship between currents and fish movement, tracks were matched with the closest ADCP measurements of zonal and meridional current velocities in time and depth.

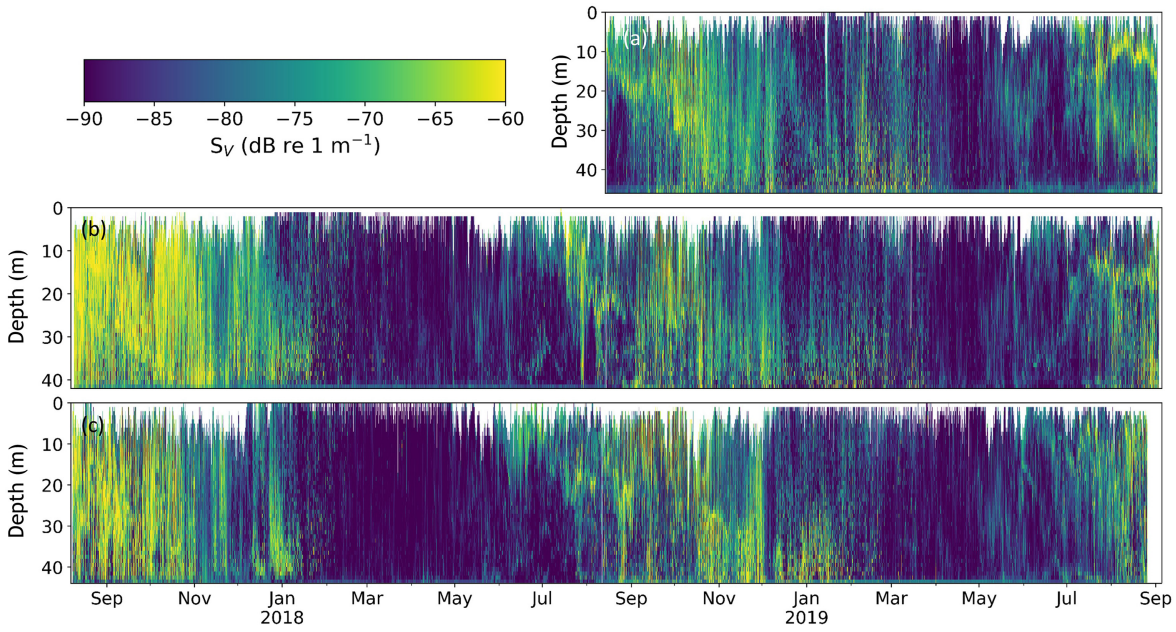

Figure 2. Echogram of 70 kHz volume backscatter recorded during each 2-h ensemble from 7 August 2017 to 6 September 2019 at the (a) northern, (b) central, and (c) southern moorings. Each point represents the mean of all observations in a 1-m depth bin of the water column recorded every 2 h. White portions of the echogram indicate areas where backscatter from the sea surface and/or sea ice have been removed.

To explore patterns in fish abundance relative to seasonal changes in sea ice, sea ice concentrations were obtained from the NOAA/NSIDC Climate Data Record of Passive Microwave Sea Ice Concentration, Version 3 (Peng *et al.*, 2013; Meier *et al.*, 2017). Daily measurements were extracted from the 25 km by 25 km grid cell that contained each mooring site. The NCEP/NCAR reanalysis (Kalnay *et al.*, 1996) wind forecasts were used to estimate the wind speed and direction to compare currents and fish transport with wind forcing. Near-surface (0.995 sigma level) values of zonal and meridional wind, available in 6-h intervals, were obtained from the 2.5° grid cell nearest to the central mooring.

Results

Seasonality of acoustic backscatter

Acoustic backscatter was greatest during the late summer and early fall, decreasing in the winter and all deployments. Relatively high backscatter values first developed in the upper water column in early summer and then extended deeper during both summers (Figure 2), indicating that the distribution of strong scatterers (i.e. fishes) moved deeper in summer. Previous work has identified evidence of low-magnitude diel vertical migration, at least on a seasonal basis (Levine, 2021; Levine *et al.*, 2021). Overall, backscatter tended to be higher at night than during the day (daily mean ± SD of $[\overline{s_{A,Night}} - \overline{s_{A,Day}}]/\overline{s_A}$ was 9 ± 67% at the southern mooring, 17 ± 65% at the central mooring, and 10 ± 72% at the northern mooring), likely associated with night-time upward movement of scatterers into the observed area.

The difference in volume backscatter observed at 70 and 200 kHz ($\Delta S_{v,70-200}$, Figure 3) exhibited strong seasonal changes, indicating seasonal shifts in the composition of scatterers. In late winter and spring, when backscatter was low (Figure 2), $\Delta S_{v,70-200}$ was consistent with zooplankton-like scatterers at all three sites (blue regions, Figure 3). Fish-like scatterers (red regions, Figure 3) appeared concurrently with the increase in backscatter in early summer (Figure 2). The greatest backscatter occurred during periods when $\Delta S_{v,70-200}$ indicated that the backscatter was dominated by fish-like scatterers (Supplementary Figure S4), consistent with previous survey observations of small fishes dominating pelagic backscatter in summer (De Robertis *et al.*, 2017; Levine *et al.*, 2023). While $\Delta S_{v,70-200}$ was consistent with scattering from fish ($\Delta S_{v,70-200} > -3$ dB) in only 41.0–62.4% of the 22660 ensembles measured across all deployments, those ensembles occurred during high-abundance periods, accounting for 84.0–97.8% of total backscatter in each deployment (Table 1). Similarly, mean *TS* was consistent with the expectation for age-0 gadids (*TS* > -62 dB re 1 m^2) 60.2–81.7% of the time (represented by the black regions in the threshold indicator above each echogram, Figure 3), and the majority (>93%) of the backscatter was observed during these periods. Although there were periods where low *TS* and frequency response indicated that backscatter was likely dominated by scatterers other than swimbladdered fishes, these periods accounted for a relatively low proportion of the total backscatter. Thus, the analyses presented below interpret s_A during periods of high backscatter as a proxy for the abundance of pelagic fishes.

Seasonal changes in fish size and abundance

There was strong seasonality in the backscatter consistent with scattering from fish at all three mooring sites (Figure 4). Backscatter began to increase in July in both 2018 and 2019, peaking in the fall. Target strengths during this period were consistent with previous observations of scattering from age-0 gadids (*TS* ~ -55 dB re 1 m^2 for 5 cm fork length, Geoffroy *et al.*, 2016; Figure 4b, d, and f), further supported by the observations of $\Delta S_{v,70-200} > 0$ indicating the presence of fishes (Figure 3). Intra-track variability in *TS* was low (Supplementary Figure S5a), and the mean *TS* of tracks was consistent throughout most of the water column with little

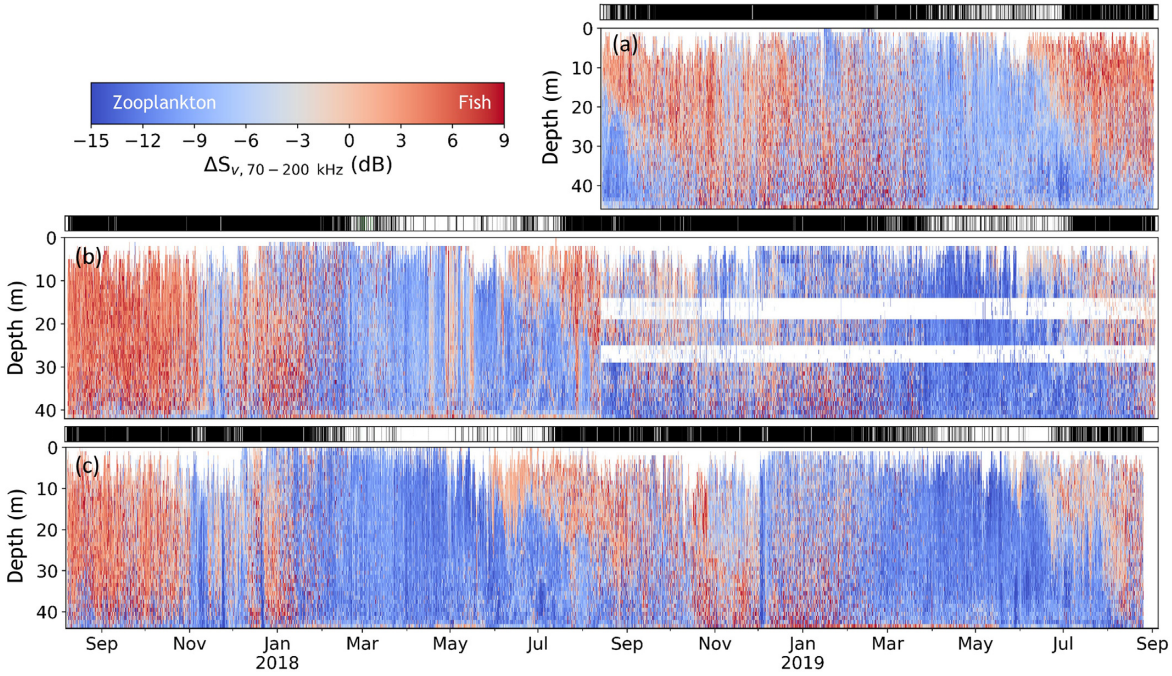

Figure 3. Echogram of the difference between 70 and 200 kHz volume backscatter ($\Delta S_{V,70\text{-}200\ kHz}$, dB) at the (a) northern, (b) central, and (c) southern moorings. Red indicates bins where Sv is greater at 70 kHz (fish-like scatterers), and blue indicates bins where S_V is greater at 200 kHz (zooplankton-like scatterers). Each point represents the mean of all observations in a 1-m depth bin of the water column recorded every two hours. White portions of the echogram indicate areas of no data due to the removal of backscatter from the sea surface and ice. Due to interference between 16–20 and 27–30 m depth at 200 kHz at the central site during the 2018–2019 deployment, data where the signal was <10 dB higher than the noise level were removed (see Methods). The black regions in the bars above each echogram indicate when the mean water column *TS* was consistent with scattering from fish (*TS* > -62 dB re 1 m^2, see Methods for details).

Table 1. Percent of ensembles, total backscatter, and total flux where *TS* and frequency response ($\Delta S_{v,70\text{-}200\ kHz}$) were consistent with scattering from gadids for each deployment.

Deployment	Site	% of Ensembles		% of Backscatter		% of Flux	
		$\Delta S_{v,70-200}$ > -3	TS > -62	$\Delta S_{v,70-200}$ > -3	TS > -62	$\Delta S_{v,70-200}$ > -3	TS > -62
2017–2018	Southern	46.9	60.2	96.3	95.8	93.3	83.1
	Central	62.4	68.1	97.8	97.7	95.6	90.3
2018–2019	Southern	41.0	71.1	84.0	93.9	75.3	68.7
	Central	55.7	77.5	89.8	96.7	81.3	80.3
	Northern	62.2	81.7	89.1	95.0	83.1	75.0

Thresholds for *TS* (*TS* > -62 dB re 1 m^2) and frequency response ($\Delta S_{v,70-200}$ > -3) were selected based on the distribution of mooring observations collected during acoustic-trawl surveys in August and September of 2017 and 2019 (Supplementary Figure S3), when age-0 gadids dominated the pelagic backscatter (Levine *et al.*, 2023; see Methods for details).

evidence of depth-dependent variation in size (Supplementary Figure S5b). There were very few observations of *TS*s consistent with larger fishes (e.g. *TS* ~ -35 dB re 1 m^2 for a 35 cm adult pollock, Traynor, 1996) throughout the deployments (Supplementary Figure S6). Backscatter was highest at all sites when bottom temperatures were >1°C (Figure 5a), which occurred in late summer and fall (Figure 4a, c, and e).

Backscatter decreased as sea ice concentration over the moorings increased in November and December (Figure 4a, c, and e). Mean backscatter was ~3–8 times lower at all three mooring sites when sea ice concentration was >20% (*t*-test on log-transformed 70 kHz s_A, $p < 0.001$ at all sites, Figure 5b). However, *TS*s remained consistent, indicating that fish of similar size were still present, though in reduced numbers (Figure 4b, d, and f).

Backscatter was very low at all three sites during winter, and lowest during spring (March–May; Figure 4a, c, and e, Supplementary Figure S7). *TS*s also decreased substantially during the spring, likely reflecting a transition in sound scatterers from small swimbladdered gadids to a zooplankton-dominated pelagic community with lower *TS*s (Figure 4b, d, and f). The change in the frequency response also supports this inference; lower $\Delta S_{v,70-200}$ values indicative of zooplankton occurred throughout the water column from approximately March to May of both years (Figure 3). Bottom temperatures and backscatter increased after the sea ice retreated in May. Fish-like scatterers with greater *TS* began to appear in June and July (Figure 4). Their appearance was consistent with an increase $\Delta S_{v,70-200}$ initially occurring near the surface and subsequently increasing in depth over the summer (Figure 3).

Fish movements

Tracks and ACDP measurements of currents indicate that fishes were moving largely as passively advected particles. A

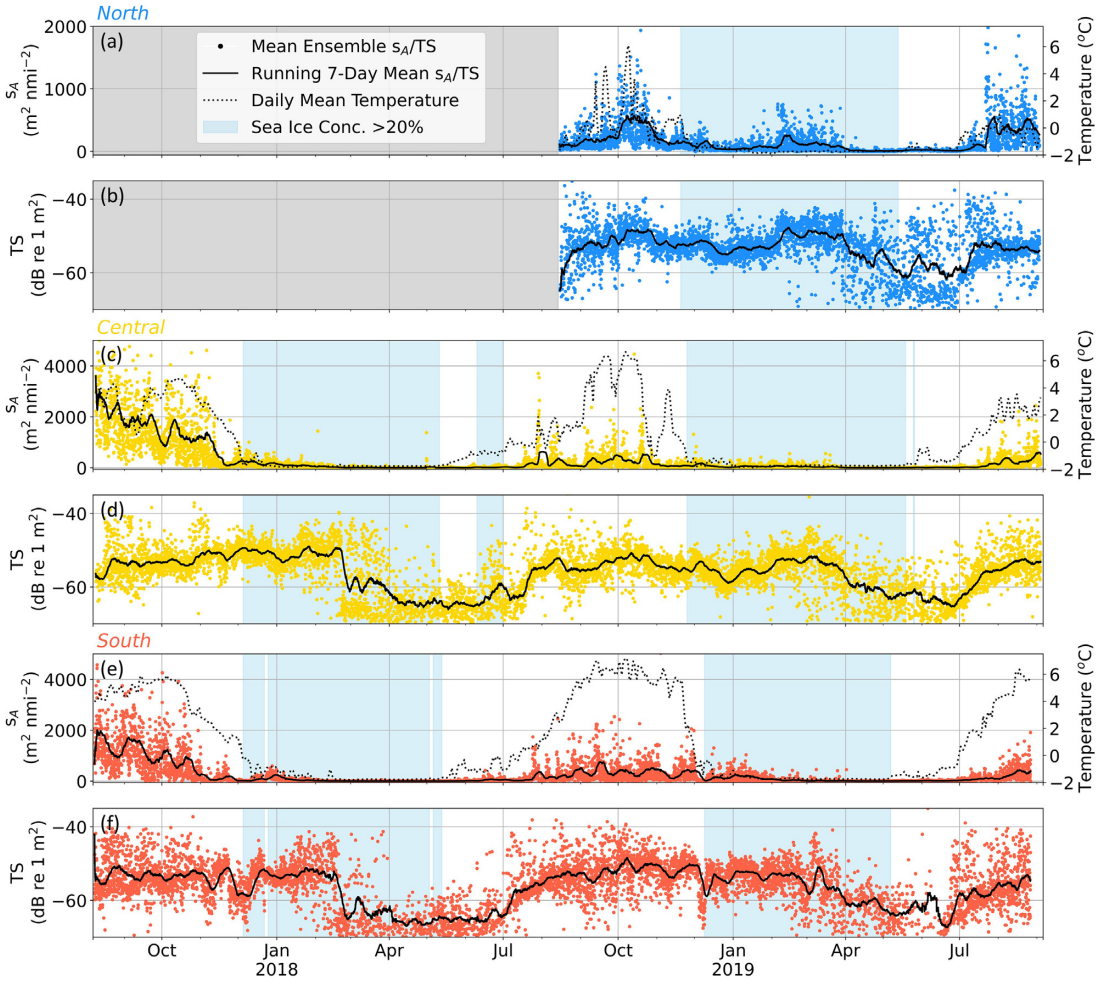

Figure 4. Time series of backscatter and environmental conditions at the (a–b, blue) northern, (c–d, yellow) central, and (e–f, red) southern mooring sites. The mean of each 2-h ensemble (points) and running 7-d mean (black line) of (a, c, and e) water column 70 kHz nautical area scattering coefficient (s_A, m^2 nmi^{-2}), and (b, d, and f) 70 kHz *TS* are shown. The bottom temperature recorded on the mooring platform is shown on the time series of s_A (a, c, e, and dotted black line). Blue shading indicates periods when sea ice concentration was >20% in the nearest 25 km^2 grid cell of satellite observations. Due to instrument failure, data are not available for the northern mooring site from the 2017–2018 deployment (a–b, grey region).

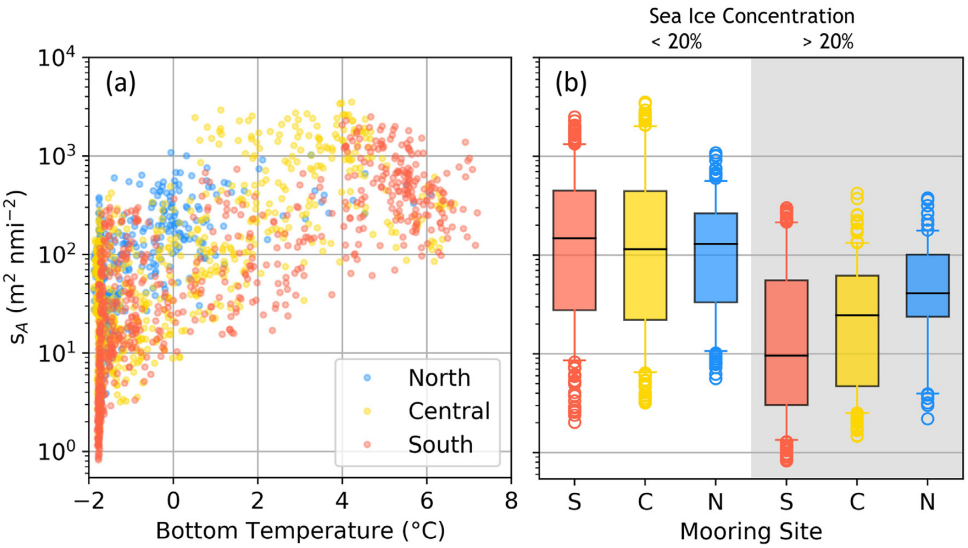

Figure 5. (a) Mean daily 70 kHz nautical area scattering coefficient (s_A, m^2 nmi^{-2}) as a function of temperature at the northern (blue), central (yellow), and southern (red) mooring sites. (b) Distributions of mean daily 70 kHz s_A when sea ice concentration was <20% (white background) and >20% (grey background). Boxes indicate the interquartile range, horizontal black lines the median, and vertical lines the 5 and 95% intervals. Circles indicate observations beyond the 5 and 95% intervals.

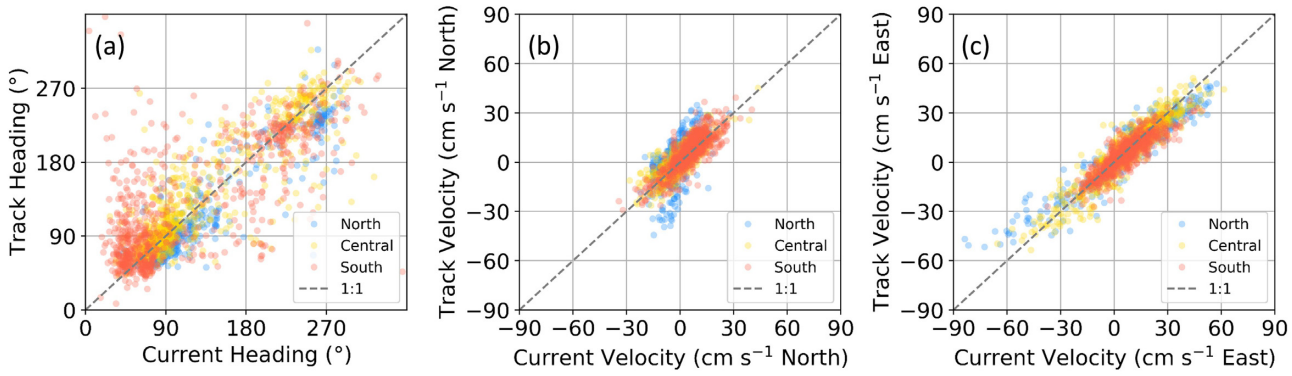

Figure 6. (a) Mean daily heading of currents measured from the Acoustic Doppler Current Profilers and tracks using the nearest depth bin of current observations for each track. Mean daily (b) zonal and (c) meridional currents and track velocities.

total of 40317, 83024, and 63674 tracks were reconstructed from single target measurements at the northern, central, and southern moorings, respectively. The mean track depth was 27 m (±10 SD; Supplementary Figure S6b, e, and h). The majority of track headings were towards the shelf break to the northeast and east, with the mean heading across all observations at each mooring (where 0° = north) at 39° (southern), 80° (central), and 87° (northern). The daily mean track heading was correlated with the current direction ($r^2 = 0.58$, $p < 0.001$, Figure 6a). Two modes were apparent in the current and track headings, corresponding to movement to the northeast and southwest (Figure 6a). The mean speed of all individual tracks was 23 (±14 SD) cm s^{-1}. Daily mean track velocities and current velocities for each site were correlated (meridional: $r^2 = 0.68$, $p < 0.001$, Figure 6b; zonal: $r^2 = 0.74$, $p < 0.001$, Figure 6c), and the track and current velocities were not significantly different (*t*-test, $p < 0.01$), suggesting individuals were passively moving with the current.

Although there are periods when the backscatter appears to be dominated by scatterers other than fish (Table 1, Figure 3), the majority of the observed flux occurred when *TS* and frequency responses indicated fish were inferred to be the dominant scatterers (Table 1). Flux estimates were greatest during the summer and fall when *TS* was consistent with fish and lowest during ice-covered periods when fish were likely scarce (Figures 4 and 7). Flux was primarily to the northeast and east at all three sites (Figures 7 and 8, Table 2), indicating net transport towards the shelf break. Mean flux estimates were highest at the central site in 2017–2018 and the northern site in 2018–2019, and lowest at the southern site in both years (Table 2). The highest mean flux over a 7-d period was 2.6 individuals m^{-1} s^{-1}, which was observed in September 2017 at the central mooring site (Figure 7b). This corresponds with the highest backscatter observed throughout the deployments (Figure 4c).

Mean flux estimates indicate that over longer timescales, fish were consistently transported to the northeast (Table 2, Figure 8). However, short episodes of movement to the southwest occurred throughout the year (Figure 7). These reversals were associated with shifts in the current, likely driven by wind speed and direction (Figure 9). Daily mean estimated wind velocities during the deployment period ranged from -13.5 to 19.9 m s^{-1} (mean of -0.05 m s^{-1} ± 5.5 SD) to the north and -15.0 to 12.1 m s^{-1} (mean of -3.0 m s^{-1} ± 5.1 SD) to the east. When wind velocities to the north and east were high, tracks primarily moved to the northeast/east (Figure 9). Fish headings became more variable as winds weakened, and fish movement to the southwest occurred more frequently as wind velocities increased towards the south and west (Figure 9).

Discussion

Seasonality of fishes

The two years of observations from moored echosounders provide evidence of strong seasonality in the abundance of the pelagic fish community on the eastern Chukchi shelf. Large numbers of age-0 gadids have been observed in the summer (De Robertis *et al.*, 2017; Levine *et al.*, 2023). However, few age-1+individuals were observed in these surveys, indicating that either mortality in this region was high or that these fishes emigrated to other regions. In the northeastern Chukchi Sea, we found that the age-0 gadids appeared in late summer and disappeared in early winter. This strong seasonality was consistent with previous observations of high abundances of pelagic organisms on the Chukchi Sea shelf in summer (Kitamura *et al.*, 2017; Gonzalez *et al.*, 2021). Tracking of fish targets revealed that fish movements were largely driven by local currents, and flux estimates indicated that the majority of the age-0 population in summer was likely transported to the northeast and east towards the Beaufort Sea and Arctic Basin each fall and winter. These findings suggest that these small fishes are transported much like passive particles, supporting the inferences drawn from passive particle tracking simulations, which predict the displacement of the summer age-0 population to the northeast off the Chukchi shelf in fall (Levine *et al.*, 2021).

The presence of fishes appears to be strongly associated with warm water entering the region. Temperature is a key driver of both Arctic cod and pollock distributions (Sigler *et al.*, 2017; Eisner *et al.*, 2020; Baker, 2021; Levine *et al.*, 2023) and growth (Laurel *et al.*, 2018). The northward transport of warm Bering Sea water in spring and summer into the northeastern Chukchi Sea (Danielson *et al.*, 2017) has been associated with increases in abundance of zooplankton (Eisner *et al.*, 2013; Ashjian *et al.*, 2017; Spear *et al.*, 2020) and fishes (Logerwell *et al.*, 2020; Levine *et al.*, 2023). High abundances of fishes in the northeastern Chukchi Sea in summer appear to coincide with southern-origin water masses. These flow north into the Chukchi Sea from the Bering Sea shelf (Coachman *et al.*, 1975; Danielson *et al.*, 2017) and replace the colder

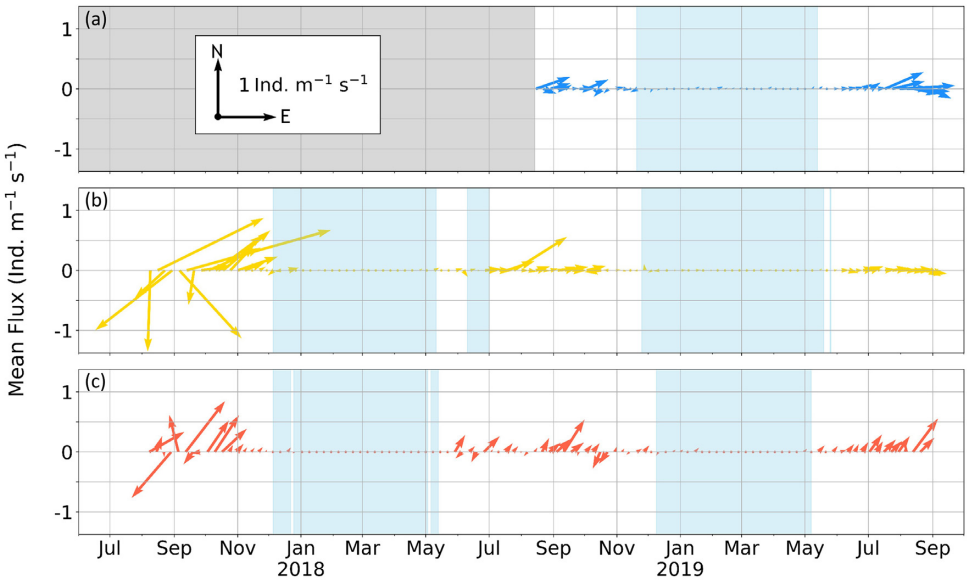

Figure 7. Mean flux of individuals (ind. m^{-1} s^{-1}) at the (a) northern, (b) central, (c) and southern mooring sites. Each arrow indicates the mean flux during a single week of deployment. The direction of the arrow indicates the mean direction of the flux, with north and east being to the top and right, respectively, as shown in the key. The length of the arrow represents the number of individuals per second in the entire water column moving underneath a 1 m line of the sea surface perpendicular to the direction of the arrow. The lengths of the arrows in the key represent a flux of 1 ind. m^{-1} s^{-1} to the north and east.

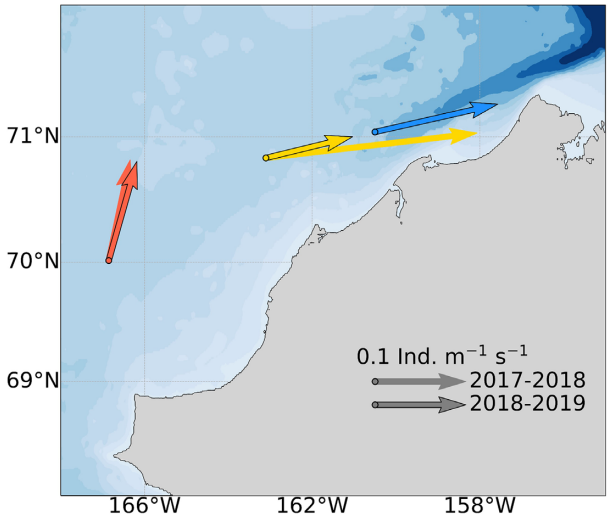

Figure 8. Map of the northeastern Chukchi Sea shelf showing the mean flux over each deployment at the northern (blue), central (yellow), and southern (red) mooring sites. The circles at the base of each arrow indicate the location of the mooring. The direction of each arrow indicates the mean direction of the flux, and the length represents the magnitude of the flux. The arrows in the key represent values of 0.1 individuals m^{-1} s^{-1}. 2017–2018 deployments are indicated by the solid colour arrows, and 2018–2019 deployments are indicated by the outlined arrows.

winter water on the Chukchi shelf (Weingartner *et al.*, 2013). The age-0 gadids observed in the northeastern Chukchi in summer are primarily associated with the warmer (2–8 °C) conditions of these seasonal water masses (De Robertis *et al.*, 2017; Marsh *et al.*, 2020; Levine *et al.*, 2023). The observations in this study provide direct evidence that the seasonality of age-0 gadids in the northeastern Chukchi Sea is driven by the advective movement of the fish population within this warmer water.

Fish abundance was higher in the summer and fall of 2017 than in the following two years at the central and southern sites. This high interannual variability is consistent with survey observations of substantially greater age-0 gadid abundances in 2017 than in 2018 and 2019 (Levine *et al.*, 2021; Levine *et al.*, 2023). Levine *et al.*, (2023) hypothesize that this increase in gadids was associated with the anomalously warm conditions in spring 2017, resulting in earlier hatching and favourable growth conditions that led to increased length-at-age and thus increased age-0 fish survival.

While it was not possible to directly assess fish sizes, the acoustic backscatter measurements strongly support previous observations that the pelagic community in summer is dominated by small fishes. Mean *TS*s during periods dominated by fish-like scattering were consistent with the *TS* expected from a mixture of small (<6 cm) age-0 Arctic cod and pollock (Traynor, 1996; Geoffroy *et al.*, 2016; Levine *et al.*, 2021). While the reported *TS*-length relationships for age-0 gadids are from ship-based (dorsal) observations at 38 kHz (Traynor, 1996; Geoffroy *et al.*, 2016), inferred lengths from mooring observations are ventral measurements collected at 70 kHz. However, intercalibration of these observations in previous work have shown that the difference between upward-facing moorings and ship-based observations is likely small for walleye pollock (~1 dB, De Robertis *et al.*, 2018); we therefore applied the *TS*-length relationships estimated at 38 kHz to observations at 70 kHz as a first approximation. The variability between dorsal and ventral measurements of the same orientation is low relative to changes in tilt angle (Francis and Foote, 2003). The ratio of vertical to horizontal movement, calculated from the maximum difference in depth among targets within a track, was <0.17 in 90% of tracks, corresponding to a tilt angle of <10°. Variability in *TS* as a result of these low tilt angles would likely not account for substantial reduction in *TS* of gadids such that larger fish would be artificially undersampled (Hazen and Horne, 2004). Even with these

Table 2. Mean direction and flux estimates (individuals m^{-1} s^{-1}) over each deployment.

Deployment	Site	Mean Direction	Mean Flux (Ind. m^{-1} s^{-1})	Net Movement (Ind. m^{-1})
2017–2018	Southern	31°	0.11	3.6×10^6
	Central	87°	0.23	7.4×10^6
2018–2019	Southern	39°	0.11	3.7×10^6
	Central	85°	0.09	3.2×10^6
	Northern	85°	0.13	4.5×10^6

Net movement (ind. m^{-1}) indicates the estimated number of individuals passing under a 1-m line on the sea surface perpendicular to the mean heading during the ~1-year duration of the mooring deployment (see Methods for additional details).

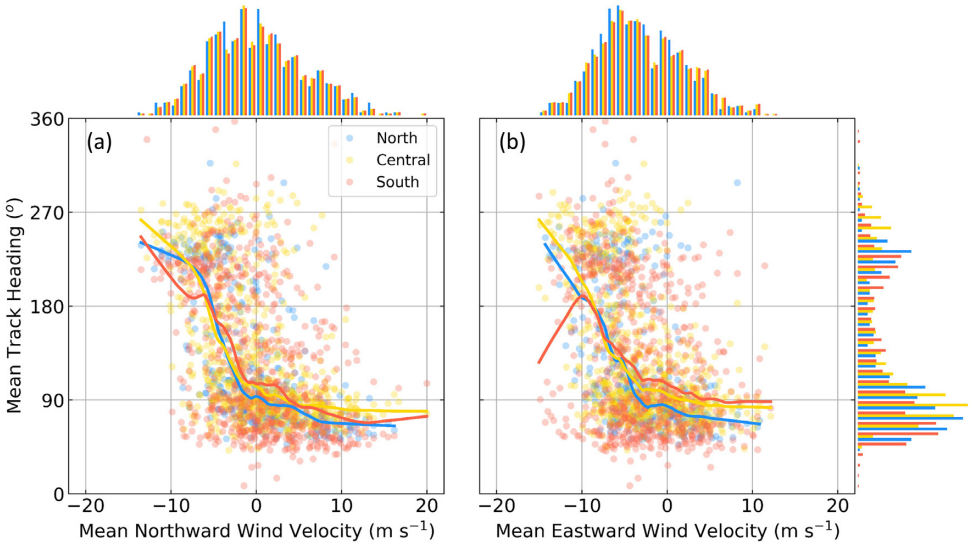

Figure 9. Daily mean track heading as a function of daily mean (a) meridional and (b) zonal wind velocities at the northern (blue), central (yellow), and southern (red) mooring sites. Histograms represent the distribution of wind velocity (top) and fish headings (right) for both years of deployments at each mooring site. The solid lines represent a locally estimated scatterplot smoothing curve (Cleveland, 1979) of the daily means for each mooring to indicate the trend.

potential sources of variability, the scarce observations of high (> -40 dB re 1 m^2) *TS*s (Supplementary Figures S3 and S6) indicate that larger gas-bearing pelagic fishes such as adult pollock were not abundant.

Transport of age-0 gadids

Fish headings and velocities were similar to those of the water, suggesting that fishes on the northeastern Chukchi shelf mostly drift with the currents. While age-0 gadids are capable of fast swimming speeds [aerobic threshold of 2–3 body lengths s^{-1} (10–15 cm s^{-1} for a 5 cm fish), Hurst, 2007; Kunz *et al.*, 2018], routine speeds are much slower [0.25–1 body lengths s^{-1} (1.25–5 cm s^{-1} for a 5 cm fish), Rose *et al.*, 1995; Hurst, 2007]. In the current velocities observed on the Chukchi shelf [mean speed of 19.9 (range of 0.2–105.2) cm s^{-1} across all sites with >95% of current observations across all sites >5 cm s^{-1}], routine swimming behaviour is likely to result in minimal displacement relative to advection. Our *in situ* observations support the assumption of passive drifting usually employed in models of the horizontal distribution of age-0 gadids in summer (Deary *et al.*, 2021; Vestfals *et al.*, 2021). This work provides further evidence that future studies can use physical observations (e.g. ADCPs) or model predictions of regional transport to assess historic and future trends in the source and fate of the populations of age-0 fishes observed in summer.

The northeastward flux of age-0 fishes varied substantially between seasons and mooring locations. The variability in heading was due to local currents, while the seasonality of the magnitude of the flux at a single station was primarily driven by seasonal changes in abundance (Supplementary Figure S8). During 2018–2019, the mean flux was highest at the northern site, although fish abundance was lower than the other sites. Current velocities are typically faster at the northern mooring site than the central and southern sites (Weingartner *et al.*, 2005; Woodgate *et al.*, 2005; Stabeno and McCabe, 2023), particularly in summer (Stabeno and McCabe, 2023), when we observed the highest fish abundances. Although density was comparable between the southern and central sites (Figure 4), fluxes were lowest in both years at the southern site (Figure 7). This variability in flux is likely due to the slower velocities typically observed in this portion of the shelf compared to velocities closer in proximity to Barrow Canyon (Woodgate *et al.*, 2005; Stabeno and McCabe, 2023).

The flux of fishes to the northeast suggests that the age-0 fishes present in summer are transported out of the shallow northeastern Chukchi shelf by their first winter, consistent with particle tracking simulations based on models of regional advection (Levine *et al.*, 2021). The flux at the northern mooring site could account for a significant portion of the export of age-0 fishes from the shelf. Extrapolating the estimated flux of 4.5×10^6 fish m^{-1} in a one-year deployment (Table 2) to a ~35 km line at the northern site would account for the

annual export of ~1.5 × 10^{11} fishes, the total number reported in the 2019 survey (Levine *et al.*, 2023). This distance represents ~10% of the eastern (U.S.) portion of the Chukchi shelf at 71 °N. Summer surveys indicate that these fishes exist in a relatively uniform distribution when abundances are high (i.e. large-scale scattering layers rather than discrete schools; De Robertis *et al.*, 2017; Levine *et al.*, 2023), and both shipboard and moored observations find that flow in the northeastern Chukchi Sea is highly uniform across the shelf (Danielson *et al.*, 2017; Stabeno and McCabe, 2023). Thus, the backscatter observed by the moorings very likely represents abundance patterns over a much broader spatial area than solely the small area of the acoustic beam sampled directly (Brierley *et al.*, 2006; De Robertis *et al.*, 2018). Further, while extrapolation of mooring observations may only apply within appropriate depth ranges due to changes in either behaviour or advection (De Robertis *et al.*, 2018), the eastern Chukchi shelf has a relatively consistent depth, suggesting the mooring results may be representative of a larger area.

The low abundance of adult Arctic cod in previous midwater and demersal surveys leads us to hypothesize that advection out of the region is the most likely explanation for the observed low numbers of adult fish. Age-1+Arctic cod have been found during recent demersal surveys of the Chukchi shelf in summer (Norcross *et al.*, 2013; Goddard *et al.*, 2014; Logerwell *et al.*, 2017), though at much lower densities than pelagic estimates (De Robertis *et al.*, 2017; Levine *et al.*, 2023). The presence of age-1+fish along the seafloor suggests that Arctic cod become more demersal as they age (and thus potentially less detectable by the upward-looking echosounders). However, our observations indicate that these age-0 fish may be advected out of the area before settling, suggesting that very few of these young fish likely transition to a demersal life history stage within the northeastern Chukchi Sea (De Robertis *et al.*, 2017; Levine *et al.*, 2021).

The very low densities of age-1+gadids on the Chukchi shelf (De Robertis *et al.*, 2017; Levine *et al.*, 2023) also suggest that the age-0 fishes found in the eastern Chukchi Sea likely originated in other areas. Previous studies using models have hypothesized that the distribution of age-0 fishes observed in summer and fall reflects the northward advection of fishes from spawning areas in the Bering Strait region (Deary *et al.*, 2021; Vestfals *et al.*, 2021). The mooring observations are consistent with this hypothesis: While this study did not identify specific spawning locations, we infer from the strong correlation between fish displacement and currents that age-0 gadids in the Chukchi during summer are likely of southern origin, following the transport pathway of water from the Bering Sea into the Arctic. Larger fish, however, are less likely to be passively transported with their drifting eggs and may maintain their position in their preferred habitat. Age-1+fishes have also likely developed the swimming ability required to return to spawning grounds. While we did not observe high *TS* tracks migrating south consistent with the return of large fishes to spawning grounds in the observations, some portion of the age-0 population may be returning as mature adults to maintain the spawning population, possibly in areas farther offshore (Forster *et al.*, 2020).

Whether the age-0 fishes that we observed in the Chukchi Sea survive over winter after drifting into the Arctic remains unclear. While Arctic cod are adapted to tolerate the near-freezing conditions on the Chukchi shelf in winter, pollock are not (Koenker *et al.*, 2018; Laurel *et al.*, 2018). Age-0 pollock captured during recent summer surveys of the Chukchi Sea probably did not have sufficient lipid reserves to survive the Arctic winter (Copeman *et al.*, 2022). It is thus unclear whether the observed northward flux of age-0 pollock will translate to the establishment of permanent Arctic populations. In contrast, Arctic cod are widely present throughout the Arctic basin and are capable of surviving in Arctic winter conditions. Aggregations of age-1+Arctic cod have been observed at depth in Barrow Canyon (De Robertis *et al.*, 2017) and the Beaufort Sea shelf break (Parker-Stetter *et al.*, 2011; Rand and Logerwell, 2011). These age-1+fish may recruit from the age-0 Arctic cod being transported off of the Chukchi shelf. This likely connectivity between these populations is further supported by the genetic similarity between Arctic cod in the Chukchi and western Beaufort Seas (Wilson *et al.*, 2019; Nelson *et al.*, 2020). Further work is necessary to identify whether the Chukchi and western Beaufort slopes are the wintering grounds for the majority of the age-0 Arctic cod observed on the Chukchi shelf in winter.

Winds influence fish transport

The direction of fish movements appears to be driven primarily by changes in current speed and direction. On the Chukchi shelf, the prevailing flow is to the north (Woodgate *et al.*, 2005), with variations in the current resulting from changes in wind conditions (Weingartner *et al.*, 2005; Woodgate *et al.*, 2005). The northward currents are typically restrained by winds to the southwest but can be enhanced during periods of strong winds to the northeast, and conversely, episodic flow reversals can occur during periods of strong winds to the southwest (Woodgate *et al.*, 2005; Pisareva *et al.*, 2019; Stabeno and McCabe, 2023). This wind-mediated change in flow is consistent with the observations of fish movement; during periods of weak and variable winds, fish movement remained towards the northeast (Figure 9), consistent with the expected flow on the northeastern shelf (Stabeno and McCabe, 2023). This movement was strengthened during strong north- and east-ward winds, when movement of both currents and fish was to the north/east (Figure 9, Supplementary Figure S9 yellow box). When winds were > ~6 m s^{-1} to the southwest, current and fish movement reversed, with a higher proportion of fish moving to the south/west (Figure 9, Supplementary Figure S9 purple box). This periodic reversal is consistent with reports that >6 m s^{-1} winds towards the southwest result in a transition from northerly to southerly flow (Fang *et al.*, 2017). These reversals are hypothesized to increase retention on the shelf and influence the late-summer distribution of age-0 fishes in the Chukchi Sea (Levine *et al.*, 2021; Vestfals *et al.*, 2021).

Transport into the Chukchi Sea has been increasing over recent decades, considerably reducing the time needed to flush and renew the water on the Chukchi shelf (Woodgate, 2018). Based on the mean fish track velocity of 8.2 cm s^{-1}, the residence time of fish on the Chukchi shelf is ~85 d (assuming ~600 km of transit from Bering Strait to Barrow Canyon). This study occurred during a period of high transport relative to previous decades (Woodgate and Peralta-Ferriz, 2021; Levine *et al.*, 2023), which may have decreased the residence time of age-0 gadids on the Chukchi shelf. This may have negative consequences for the overwinter survival of these age-0 fishes, as feeding on the Chukchi shelf in summer is likely important for energy acquisition (Levine *et al.*, 2021).

Conclusions

The abundance and composition of the pelagic fish community on the Chukchi shelf are highly seasonal. While age-0 fishes are abundant in summer, abundance in winter is low. This study provides direct evidence that the abundant age-0 gadids observed on the Chukchi shelf in summer are only temporary residents of the region. These fishes originate from the south and drift northward across the shelf with the prevailing currents. However, transport in the region is changing, with potential consequences for the future of this ecosystem and the structure of the summer pelagic fish community. Enhanced transport from the south may be driving the increased presence of boreal species such as pollock in the eastern Chukchi Sea (Levine *et al.*, 2023). While these southern species likely cannot survive over the winter in Arctic conditions, their increased presence during summer may increase competition with, and predation on, endemic species, further altering the structure of the summer community. The identification of the role of advection in structuring this seasonal population presents opportunities for observations and predictions of the physical environment to provide insight into how this ecosystem may be restructured with continued change.

Acknowledgements

This manuscript is a product of the North Pacific Research Board Arctic Integrated Ecosystem Research Program (https://www.nprb.org/arctic-program); NPRB publication number ArcticIERP-51. We thank Phyllis Stabeno for providing us with the ADCP data, Christian Meinig and Steven Anderson for their work in the design and construction of the mooring platform, and Matthew Casari for development of the underwater compasses. We also thank Rebecca Woodgate, Sam Urmy, and Chris Bassett for their input and comments on the early draft of this work, and the editors and anonymous reviewers for their suggestions which improved this manuscript. The mooring deployments and recoveries would not have been possible without the captains, crews, and science parties of the R/V *Ocean Starr* and USCGC *Healy*. Any use of trade, firm, or product names is for descriptive purposes only and does not imply endorsement U.S. Government. Findings of this paper do not necessarily represent the views of the National Oceanic and Atmospheric Administration.

Supplementary data

Supplementary material is available at the *ICESJMS* online version of the manuscript.

Conflict of interest

The authors declare no conflicts of interest.

Funding

Funding for the program was provided by North Pacific Research Board, the Bureau of Ocean Energy Management, the Collaborative Alaskan Arctic Studies Program, and the Office of Naval Research. In-kind support was contributed by the National Oceanic and Atmospheric Administration's (NOAA) Alaska Fisheries Science Center and Pacific Marine Environmental Laboratory, the University of Alaska Fairbanks, the U.S. Fish & Wildlife Service, and the National Science Foundation.

Author contributions

RML, ADR, and CDW conceived of the project and conducted the field work. ADR, DG, and CDW managed the funding acquisition and project administration. RML, ADR, and DG contributed to the methodology and RML led the data analysis. RML led the writing of the manuscript and all authors contributed to review and editing.

Data availability

All echosounder data, including calibration information, are available via the Water Column Sonar Data archive at the NOAA National Centers for Environmental Information (https://www.ncei.noaa.gov/products/water-column-sonar-data). ADCP datasets and additional deployment information are publically available in DataONE (southern: https://doi.org/10.24431/rw1k5ao, central: https://doi.org/10.24431/rw1k5 a.m., and northern: https://doi.org/10.24431/rw1k5at).

References

Ashjian, C. J., Campbell, R. G., Gelfman, C., Alatalo, P., and Elliott, S. M. 2017. Mesozooplankton abundance and distribution in association with hydrography on Hanna Shoal, NE Chukchi Sea, during August 2012 and 2013. Deep Sea Research Part II: Topical Studies in Oceanography, 144: 21–36.

Baker, M. R. 2021. Contrast of warm and cold phases in the Bering Sea to understand spatial distributions of Arctic and sub-Arctic gadids. Polar Biology, 44: 1083–1105.

Baker, M. R., Farley, E. V., Ladd, C., Danielson, S. L., Stafford, K. M., Huntington, H. P., and Dickson, D. M. 2020. Integrated ecosystem research in the Pacific Arctic–understanding ecosystem processes timing and change. Deep Sea Research Part II: Topical Studies in Oceanography, 177: 104850.

Benoit, D., Simard, Y., and Fortier, L. 2008. Hydroacoustic detection of large winter aggregations of Arctic cod (*Boreogadus saida*) at depth in ice-covered Franklin Bay (Beaufort Sea). Journal of Geophysical Research, 113: 1–9.

Benoit, D., Simard, Y., and Fortier, L. 2014. Pre-winter distribution and habitat characteristics of polar cod (*Boreogadus saida*). Polar Biology, 37: 149–163.

Benoit-Bird, K. J., and Lawson, G. L. 2016. Ecological insights from pelagic habitats acquired using active acoustic techniques. Annual Review of Marine Science, 8: 463–490.

Blackman, S. S. 1986. Multiple-target tracking with radar applications. Artech House, Inc., Dedham, MA. 463pp.

Brierley, A. S., Saunders, R. A., Bone, D. G., Murphy, E. J., Enderlein, P., Conti, S. G., and Demer, D. A. 2006. Use of moored acoustic instruments to measure short-term variability in abundance of Antarctic krill. Limnology and Oceanography: Methods, 4: 18–29.

Cleveland, W. S. 1979. Robust locally weighted regression and smoothing scatterplots. Journal of the American Statistical Association, 74: 829–836.

Coachman, L. K., Aagaard, K., and Tripp, R. B. 1975. Bering Strait: The Regional Physical Oceanography. University of Washington Press, Seattle. 172pp.

Copeman, L. A., Salant, C. D., Stowell, M. A., Spencer, M. L., Kimmel, D. G., Pinchuk, A. I., and Laurel, B. J. 2022. Annual and spatial variation in the condition and lipid storage of juvenile Chukchi Sea gadids during a recent period of environmental warming (2012 to 2019). Deep Sea Research Part II: Topical Studies in Oceanography, 205: 105180.

Corlett, W. B., and Pickart, R. S. 2017. The Chukchi slope current. Progress in Oceanography, 153: 50–65.

Danielson, S. L., Ahkinga, O., Ashjian, C., Basyuk, E., Cooper, L. W., Eisner, L., Farley, E., *et al.* 2020. Manifestation and consequences of warming and altered heat fluxes over the Bering and Chukchi Sea continental shelves. Deep-Sea Research Part II: Topical Studies in Oceanography, 177: 104781.

Danielson, S. L., Eisner, L., Ladd, C., Mordy, C., Sousa, L., and Weingartner, T. J. 2017. A comparison between late summer 2012 and 2013 water masses, macronutrients, and phytoplankton standing crops in the northern Bering and Chukchi Seas. Deep Sea Research Part II: Topical Studies in Oceanography, 135: 7–26.

Darnis, G., Hobbs, L., Geoffroy, M., Grenvald, J. C., Renaud, P. E., Berge, J., Cottier, F., *et al.* 2017. From polar night to midnight sun: diel vertical migration, metabolism and biogeochemical role of zooplankton in a high Arctic fjord (Kongsfjorden, Svalbard). Limnology and Oceanography, 62: 1586–1605.

David, C., Lange, B., Krumpen, T., Schaafsma, F., van Franeker, J. A., and Flores, H. 2016. Under-ice distribution of polar cod *Boreogadus saida* in the central Arctic Ocean and their association with sea-ice habitat properties. Polar Biology, 39: 981–994.

De Robertis, A., Levine, R., and Wilson, C. D. 2018. Can a bottom-moored echo sounder array provide a survey-comparable index of abundance? Canadian Journal of Fisheries and Aquatic Sciences, 75: 629–640.

De Robertis, A., McKelvey, D. R., and Ressler, P. H. 2010. Development and application of an empirical multifrequency method for backscatter classification. Canadian Journal of Fisheries and Aquatic Sciences, 67: 1459–1474.

De Robertis, A., Taylor, K., Wilson, C. D., and Farley, E. V. 2017. Abundance and distribution of Arctic cod (*Boreogadus saida*) and other pelagic fishes over the U.S. Continental Shelf of the Northern Bering and Chukchi Seas. Deep Sea Research Part II: Topical Studies in Oceanography, 135: 51–65.

Deary, A. L., Vestfals, C. D., Mueter, F. J., Logerwell, E. A., Goldstein, E. D., Stabeno, P. J., Danielson, S. L., *et al.* 2021. Seasonal abundance, distribution, and growth of the early life stages of polar cod (*Boreogadus saida*) and saffron cod (*Eleginus gracilis*) in the US Arctic. Polar Biology, 44: 2055–2076.

Demer, D. A., Berger, L., Bernasconi, M., Bethke, E., Boswell, K., Chu, D., Domokos, R., *et al.* 2015. Calibration of acoustic instruments. ICES Cooperative Research Reports 326. 133pp.

Ehrenberg, J., and Torkelson, T. C. 1996. Application of dual-beam and split-beam target tracking in fisheries acoustics. ICES Journal of Marine Science, 53: 329–334.

Eisner, L. B., Zuenko, Y. I., Basyuk, E. O., Britt, L. L., Duffy-Anderson, J. T., Kotwicki, S., Ladd, C., *et al.* 2020. Environmental impacts on walleye pollock (*Gadus chalcogrammus*) distribution across the Bering Sea shelf. Deep Sea Research Part II: Topical Studies in Oceanography, 181-182: 104881.

Eisner, L., Hillgruber, N., Martinson, E., and Maselko, J. 2013. Pelagic fish and zooplankton species assemblages in relation to water mass characteristics in the northern Bering and southeast Chukchi seas. Polar Biology, 36: 87–113.

Fang, Y. C., Potter, R. A., Statscewich, H., Weingartner, T. J., Winsor, P., and Irving, B. K. 2017. Surface current patterns in the northeastern Chukchi Sea and their response to wind forcing. Journal of Geophysical Research: Oceans, 122: 9530–9547.

Fernandes, P. G., Stevenson, P., Brierley, A. S., Armstrong, F., and Simmonds, E. J. 2003. Autonomous underwater vehicles: future platforms for fisheries acoustics. ICES Journal of Marine Science, 60: 684–691.

Flores, H., van Franeker, J. A., Siegel, V., Haraldsson, M., Strass, V., Meesters, E. H., Bathmann, U., *et al.* 2012. The association of Antarctic krill *Euphausia superba* with the under-ice habitat. PLoS One, 7: e31775.

Forster, C. E., Norcross, B. L., Mueter, F. J., Logerwell, E. A., and Seitz, A. C. 2020. Spatial patterns, environmental correlates, and potential seasonal migration triangle of polar cod (*Boreogadus saida*) distribution in the Chukchi and Beaufort seas. Polar Biology, 43: 1073–1094.

Francis, D. T., and Foote, K. G. 2003. Depth-dependent target strengths of gadoids by the boundary-element method. The Journal of the Acoustical Society of America, 114: 3136–3146.

Frey, K. E., Moore, G. W. K., Cooper, L. W., and Grebmeier, J. M. 2015. Divergent patterns of recent sea ice cover across the Bering, Chukchi, and Beaufort seas of the Pacific Arctic Region. Progress in Oceanography, 136: 32–49.

Geoffroy, M., Majewski, A., LeBlanc, M., Gauthier, S., Walkusz, W., Reist, J. D., and Fortier, L. 2016. Vertical segregation of age-0 and age-1+ polar cod (*Boreogadus saida*) over the annual cycle in the Canadian Beaufort Sea. Polar Biology, 39: 1023–1037.

Goddard, P., Lauth, R., and Armistead, C. 2014. Results of the 2012 Chukchi Sea Bottom Trawl Survey of Bottom fishes, Crabs, and Other Demersal Macrofauna. U.S Department of Commerce, NOAA Technical Memorandum NMFS-AFSC-278. Available at: https://repository.library.noaa.gov/view/noaa/4777 (last accessed 16 December 2021).

Gonzalez, S., Horne, J. K., and Danielson, S. L. 2021. Multi-scale temporal variability in biological-physical associations in the NE Chukchi Sea. Polar Biology, 44: 837–855.

Gradinger, R. R., and Bluhm, B. A. 2004. In-situ observations on the distribution and behavior of amphipods and Arctic cod (*Boreogadus saida*) under the sea ice of the High Arctic Canada Basin. Polar Biology, 27: 595–603.

Hazen, E. L., and Horne, J. K. 2004. Comparing the modelled and measured target-strength variability of walleye pollock, *Theragra chalcogramma*. ICES Journal of Marine Science, 61: 363–377.

Hurst, T. P. 2007. Thermal effects on behavior of juvenile walleye pollock (*Theragra chalcogramma*): implications for energetics and food web models. Canadian Journal of Fisheries and Aquatic Sciences, 64: 449–457.

Jech, J. M., and Michaels, W. L. 2006. A multifrequency method to classify and evaluate fisheries acoustics data. Canadian Journal of Fisheries and Aquatic Sciences, 63: 2225–2235.

Kaartvedt, S., Røstad, A., Klevjer, T. A., and Staby, A. 2009. Use of bottom-mounted echo sounders in exploring behavior of mesopelagic fishes. Marine Ecology Progress Series, 395: 109–118.

Kalnay, E., Kanamitsu, M., Kistler, R., Collins, W., Deaven, D., Gandin, L., Iredell, M., *et al.* 1996. The NCEP/NCAR 40-year reanalysis project. Bulletin of the American Meteorological Society,77: 437–471.

Kitamura, M., Amakasu, K., Kikuchi, T., and Nishino, S. 2017. Seasonal dynamics of zooplankton in the southern Chukchi Sea revealed from acoustic backscattering strength. Continental Shelf Research, 133: 47–58.

Koenker, B. L., Copeman, L. A., and Laurel, B. J. 2018. Impacts of temperature and food availability on the condition of larval Arctic cod (*Boreogadus saida*) and walleye pollock (*Gadus chalcogrammus*). ICES Journal of Marine Science, 75: 2370–2385.

Kunz, K. L., Claireaux, G., Po¨ Rtner, H.-O., Knust, R., Mark, F. C., Pörtner, H.-O., Knust, R., *et al.* 2018. Aerobic capacities and swimming performance of polar cod (*Boreogadus saida*) under ocean acidification and warming conditions. Journal of Experimental Biology, 221: jeb184473.

Laurel, B. J., Copeman, L. A., Spencer, M., and Iseri, P. 2018. Comparative effects of temperature on rates of development and survival of eggs and yolk-sac larvae of Arctic cod (*Boreogadus saida*) and walleye pollock (*Gadus chalcogrammus*). ICES Journal of Marine Science, 75: 2403–2412.

Levine, R. M. 2021. Climate-driven shifts in abundance, distribution, and composition of the pelagic fish community in a rapidly changing Pacific Arctic. University of Washington, Seattle, WA.

Levine, R. M., De Robertis, A., Grünbaum, D., Wildes, S., Farley, E. V., Stabeno, P. J., and Wilson, C. D. 2023. Climate-driven shifts in pelagic fish distributions in a rapidly changing Pacific Arctic. Deep Sea Research Part II: Topical Studies in Oceanography, 208: 105244.

Levine, R. M., De Robertis, A., Grünbaum, D., Woodgate, R., Mordy, C. W., Mueter, F., Cokelet, E., *et al.* 2021. Autonomous vehicle surveys indicate that flow reversals retain juvenile fishes in a highly advective high-latitude ecosystem. Limnology and Oceanography, 66: 1139–1154.

Logerwell, E. A., Busby, M., Mier, K. L., Tabisola, H., and Duffy-Anderson, J. 2020. The effect of oceanographic variability on the distribution of larval fishes of the northern Bering and Chukchi seas. Deep Sea Research Part II: Topical Studies in Oceanography, 177: 104784.

Logerwell, E., Rand, K., Danielson, S., and Sousa, L. 2017. Environmental drivers of benthic fish distribution in and around Barrow Canyon in the northeastern Chukchi Sea and western Beaufort Sea. Deep Sea Research Part II: Topical Studies in Oceanography, 152: 170–181.

Lønne, O. J., and Gulliksen, B. 1989. Size, age and diet of polar cod, *Boreogadus saida* (Lepechin 1773), in ice covered waters. Polar Biology, 9: 187–191.

Lowry, L. F., and Frost, K. J. 1981. Distribution, growth, and foods of Arctic cod (*Boreogadus saida*) in the Bering, Chukchi and Beaufort Seas. Canadian Field-Naturalist, 95: 186–191.

Maclennan, D. N., Fernandes, P. G., and Dalen, J. 2002. A consistent approach to definitions and symbols in fisheries acoustics. ICES Journal of Marine Science, 59: 365–369.

Marsh, J. M., and Mueter, F. J. 2020. Influences of temperature, predators, and competitors on polar cod (*Boreogadus saida*) at the southern margin of their distribution. Polar Biology, 43: 995–1014.

Marsh, J. M., Mueter, F. J., and Quinn, T. J. 2020. Environmental and biological influences on the distribution and population dynamics of polar cod (*Boreogadus saida*) in the US Chukchi Sea. Polar Biology, 43: 1055–1072.

McClatchie, S., Alsop, J., and Coombs, R. F. 1996. A re-evaluation of relationships between fish size, acoustic frequency, and target strength. ICES Journal of Marine Science, 53: 780–791.

Mecklenburg, C., Lynghammar, A., Johannesen, E., Byrkjedal, I., Christiansen, J.S., Karamushko, O. V, Mecklenburg, T.A., *et al.* 2018. Marine Fishes of the Arctic Region. Conservation of Arctic Flora and Fauna, Akureyri, Iceland. ISBN 978-9935-431-70-7.

Meier, W. N., Fetterer, F., Savoie, M., Mallory, S., Duerr, R., and Stroeve, J. 2017. NOAA/NSIDC Climate Data Record of Passive Microwave Sea Ice Concentration, Version 3. Boulder, Colorado USA. NSIDC: National Snow and Ice Data Center. Boulder, Colorado USA.

Melnikov, I. A., and Chernova, N. V. 2013. Characteristics of under-ice swarming of polar cod *Boreogadus saida* (Gadidae) in the Central Arctic Ocean. Journal of Ichthyology, 53: 7–15.

Miksis-Olds, J. L., Stabeno, P. J., Napp, J. M., Pinchuk, A. I., Nystuen, J. A., Warren, J. D., and Denes, S. L. 2013. Ecosystem response to a temporary sea ice retreat in the Bering Sea: winter 2009. Progress in Oceanography, 111: 38–51.

Mueter, F. J., Planque, B., Hunt, G. L., Alabia, I. D., Hirawake, T., Eisner, L., Dalpadado, P., *et al.* 2021. Possible future scenarios in the gateways to the Arctic for Subarctic and Arctic marine systems: II. prey resources, food webs, fish, and fisheries. ICES Journal of Marine Science, 78: 3017–3045.

Nelson, R. J., Bouchard, C., Fortier, L., Majewski, A. R., Reist, J. D., Præbel, K., Madsen, M. L., *et al.* 2020. Circumpolar genetic population structure of polar cod, *Boreogadus saida*. Polar Biology, 43: 951–961.

Norcross, B. L., Raborn, S. W., Holladay, B. A., Gallaway, B. J., Crawford, S. T., Priest, J. T., Edenfield, L. E., *et al.* 2013. Northeastern Chukchi Sea demersal fishes and associated environmental characteristics, 2009-2010. Continental Shelf Research, 67: 77–95.

Parker-Stetter, S. L., Horne, J. K., and Weingartner, T. J. 2011. Distribution of polar cod and age-0 fish in the U.S. Beaufort Sea. Polar Biology, 34: 1543–1557.

Peng, G., Meier, W. N., Scott, D. J., and Savoie, M. H. 2013. A long-term and reproducible passive microwave sea ice concentration data record for climate studies and monitoring. Earth System Science Data, 5: 311–318.

Pinchuk, A. I., and Eisner, L. B. 2017. Spatial heterogeneity in zooplankton summer distribution in the eastern Chukchi Sea in 2012–2013 as a result of large-scale interactions of water masses. Deep Sea Research Part II: Topical Studies in Oceanography, 135: 27–39.

Pisareva, M. N., Pickart, R. S., Lin, P., Fratantoni, P. S., and Weingartner, T. J. 2019. On the nature of wind-forced upwelling in Barrow Canyon. Deep Sea Research Part II: Topical Studies in Oceanography, 162: 63–78.

Ponomarenko, V. P. 2000. Eggs, larvae, and juveniles of polar cod *Boreogadus saida* in the Barents, Kara, and White Seas. Journal of Ichthyology, 40: 165–173.

Rand, K. M., and Logerwell, E. A. 2011. The first demersal trawl survey of benthic fish and invertebrates in the Beaufort Sea since the late 1970s. Polar Biology, 34: 475–488.

Renfree, J. S., Sessions, T. S., Murfin, D. W., Palance, D., and Demer, D. A. 2019. Calibrations of wide-bandwidth transceivers (WBT Mini) with dual-frequency transducers (ES38-18/200-18C) for saildrone surveys of the California Current ecosystem during summer 2018. U.S Department of Commerce, NOAA Technical Memorandum NMFS-SWFSC-608. Available at: https://repository.library.noaa.gov/view/noaa/19599 (last accessed 7 May 2019).

Rose, G. A., DeYoung, B., and Colbourne, E. B. 1995. Cod (*Gadus morhua* L.) migration speeds and transport relative to currents on the north-east Newfoundland Shelf. ICES Journal of Marine Science, 52: 903–913.

Sigler, M. F., Mueter, F. J., Bluhm, B. A., Busby, M. S., Cokelet, E. D., Danielson, S. L., De Robertis, A. *et al.* 2017. Late summer zoogeography of the northern Bering and Chukchi seas. Deep Sea Research Part II: Topical Studies in Oceanography, 135: 168–189.

Spear, A., Napp, J., Ferm, N., and Kimmel, d. 2020. Advection and in situ processes as drivers of change for the abundance of large zooplankton taxa in the Chukchi Sea. Deep Sea Research Part II: Topical Studies in Oceanography, 177: 104814.

Stabeno, P. J., and McCabe, R. M. 2023. Re-examining flow pathways over the Chukchi Sea continental shelf.Deep Sea Research Part II: Topical Studies in Oceanography, 207: 105243.

Stevenson, D. E., and Lauth, R. R. 2019. Bottom trawl surveys in the northern Bering Sea indicate recent shifts in the distribution of marine species. Polar Biology, 42: 407–421.

Traynor, J. 1996. Target-strength measurements of walleye pollock (*Theragra chalcogramma*) and Pacific whiting (*Merluccius productus*). ICES Journal of Marine Science, 53: 253–258.

Trevorrow, M. V. 2005. The use of moored inverted echo sounders for monitoring meso-zooplankton and fish near the ocean surface. Canadian Journal of Fisheries and Aquatic Sciences, 62: 1004–1018.

Urmy, S. S., Horne, J. K., and Barbee, D. H. 2012. Measuring the vertical distributional variability of pelagic fauna in Monterey Bay. ICES Journal of Marine Science, 69: 184–196.

Vestfals, C. D., Mueter, F. J., Duffy-Anderson, J. T., Busby, M. S., and De Robertis, A. 2019. Spatio-temporal distribution of polar cod (*Boreogadus saida*) and saffron cod (*Eleginus gracilis*) early life stages in the Pacific Arctic. Polar Biology, 42: 969–990.

Vestfals, C. D., Mueter, F. J., Hedstrom, K. S., Laurel, B. J., Petrik, C. M., Duffy-Anderson, J. T., and Danielson, S. L. 2021. Modeling the dispersal of polar cod (*Boreogadus saida*) and saffron cod (*Eleginus gracilis*) early life stages in the Pacific Arctic using a biophysical transport model. Progress in Oceanography, 196: 102571.

Wallace, M. I., Cottier, F. R., Berge, J., Tarling, G. A., Griffiths, C., and Brierley, A. S. 2010. Comparison of zooplankton vertical migration in an ice-free and a seasonally ice-covered Arctic fjord: an insight into the influence of sea ice cover on zooplankton behavior. Limnology and Oceanography, 55: 831–845.

Wang, M., Yang, Q., Overland, J. E., and Stabeno, P. 2018. Sea-ice cover timing in the Pacific Arctic: the present and projections to mid-century by selected CMIP5 models. Deep Sea Research Part II: Topical Studies in Oceanography, 152: 22–34.

Weingartner, T., Aagaard, K., Woodgate, R., Danielson, S., Sasaki, Y., and Cavalieri, d. 2005. Circulation on the north central Chukchi Sea shelf. Deep Sea Research Part II: Topical Studies in Oceanography, 52: 3150–3174.

Weingartner, T., Dobbins, E., Danielson, S., Winsor, P., Potter, R., and Statscewich, H. 2013. Hydrographic variability over the northeastern Chukchi Sea shelf in summer-fall 2008-2010. Continental Shelf Research, 67: 5–22.

Whitehouse, G. A., Aydin, K., Essington, T. E., and Hunt, G. L. 2014. A trophic mass balance model of the eastern Chukchi Sea with comparisons to other high-latitude systems. Polar Biology, 37: 911–939.

Wildes, S., Whittle, J., Nguyen, H., Marsh, M., Karpan, K., D'Amelio, C.,A. *et al.* 2022. Walleye Pollock breach the Bering Strait: a change of the cods in the arctic. Deep Sea Research Part II: Topical Studies in Oceanography, 204: 105165,

Wilson, R. E., Sage, G. K., Wedemeyer, K., Sonsthagen, S. A., Menning, D. M., Gravley, M. C., Sexson, M. G. *et al.* 2019. Micro-geographic population genetic structure within Arctic cod (*Boreogadus saida*) in Beaufort Sea of Alaska. ICES Journal of Marine Science, 76: 1713–1721.

Woodgate, R. A. 2018. Increases in the Pacific inflow to the Arctic from 1990 to 2015, and insights into seasonal trends and driving mechanisms from year-round Bering Strait mooring data. Progress in Oceanography, 160: 124–154.

Woodgate, R. A., Aagaard, K., and Weingartner, T. J. 2005. A year in the physical oceanography of the Chukchi Sea: moored measurements from autumn 1990-1991. Deep-Sea Research Part II: Deep Sea Research Part II: Topical Studies in Oceanography, 52: 3116–3149.

Woodgate, R. A., and Peralta-Ferriz, C. 2021. Warming and freshening of the Pacific inflow to the Arctic from 1990-2019 implying dramatic shoaling in Pacific Winter Water ventilation of the Arctic water column. Geophysical Research Letters, 48: e2021GL092528.

Woodgate, R. A., Weingartner, T., and Lindsay, R. 2010. The 2007 Bering Strait oceanic heat flux and anomalous Arctic sea-ice retreat. Geophysical Research Letters, 37: L01602.

Handling Editor: Alina Wieczorek